Microscopy with an infinite depth of field

D. Weigel, A. Kießling, R. Kowarschik
Institute of Applied Optics, Abbe Center of Photonics,
Center for Medical Optics and Photonics
Friedrich Schiller University Jena

FSU Jena

institute iao of applied optics

Introduction

Conventional optical imaging allows only one plane to be imaged sharply from the object space onto the image plane. As shown in Fig.1, a point with a distance Δz to the object plane will be imaged with a distance $\Delta z'$ to the image plane. Due to the 3D point spread function (PSF), only a blurred image can be observed.
Obviously, the depth information is encoded by the wave-front curvature and the lateral position is determined by its tilt. Therefore, if all wavefront curvatures can be removed without influencing the tilts or limiting the aperture of the microscope objective, all object points would be imaged onto the same plane. This would be equivalent to an infinite depth of field.
Using an image inverting interferometer (III) [1] it is possible to gain an infinite depth of field (DOF) [2].

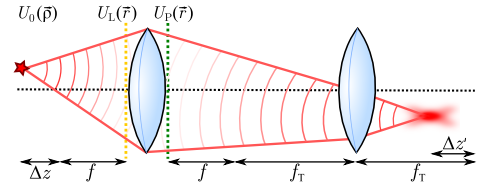

Fig.1 Scheme of a conventional infinity corrected microscope.

Theory

The basic principle of the presented coherence imaging microscope is to measure the coherence function Γ of a spatially incoherent object in the exit pupil (EP) of the microscope objective (MO) (Fig.2). Therefore, the EP is imaged through the III into the detection plane.

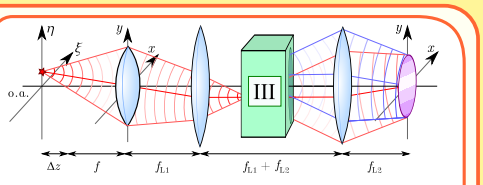

Fig.2 Scheme of a *coherence imaging microscope*. The III is represented by a "black box".

In the context of the paraxial approximation, the amplitude distribution $U_P(\vec{r},t)$ in the EP of the MO can be expressed by:

$$U_P(r,t) = P(\vec{r}/R) \cdot \frac{e^{i\frac{k}{2(f+\Delta z)}\vec{r}^2}}{i\lambda(f+\Delta z)} \cdot e^{-i\frac{k}{2f}\vec{r}^2} \cdot \mathcal{F}\left\{U_0(\rho,t) \cdot e^{i\frac{k}{2(f+\Delta z)}\vec{\rho}^2}\right\}$$

pupil · defocus · lens · Fourier transform

Due to the III, $U_P(\vec{r},t)$ interferes with its spatially inverted copy $U_P^*(-\vec{r},t)$ at the detector. The real part of the interference pattern can be interpreted as Γ. Using monochromatic light, the complex Γ can be gained by at least three phase steps. As shown in [2], Γ is independent from Δz, except for a scaling factor. By an inverse Fourier transform, the intensity $I(\rho)$ can be reconstructed. As there is no defocus term in Γ, the point spread function (PSF) does not depend on Δz, either. Therefore, all planes of the object space are reconstructed sharply.

$$\Gamma(\Delta\vec{r}) = \left\langle U_P(\vec{r},t) \cdot U_P^*(-\vec{r},t) \right\rangle_t$$

Fourier transform:

$$\Gamma(\Delta\vec{r}) = \frac{1}{\lambda^2(f+\Delta z)^2} \cdot P(\vec{r}/R) \cdot \mathcal{F}\left\{I(\vec{\rho})\right\}$$

$$I_R(\vec{\rho}) = \frac{1}{\lambda^2(f+\Delta z)^2} \cdot \frac{J_1(2\vec{\rho})}{|2\vec{\rho}|} \otimes I(\vec{\rho})$$

image · scaling factor · PSF · object

Setup

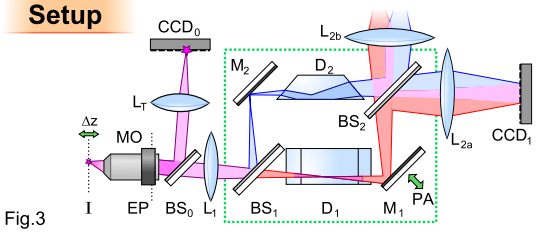

Fig.3

Sketch of the setup. As a spatially incoherent test object, the anode (grid structure) of a red LED was used. It was demagnified by an illumination MO into the object plane of the detection MO. By varying the magnification factor, different grid sizes could be realized. The illumination MO was mounted on a stepper motor. Hence, different distances Δz to the focal plane of the detection MO (NA = 0.07, 2.5x) could be applied. Note that for reasons of clarity the illumination MO as well as the light source (LED, $\lambda \approx 633$ nm) is not shown. The exit pupil (EP) of the detection MO was imaged by the lenses L_1 and L_{2a} through the III onto the detector CCD_1. The Dove prisms D_1 and D_2 are rotated by 90° to each other, leading to the required image inversion. The piezo-actuator PA is used to adjust the optical path difference between the two arms of the III. With the help of the tube lens L_T and CCD_0, the conventional control image can be taken.

Results

The PSF of the presented coherence imaging microscope is a BSinc function, which is independent from Δz. Therefore, besides the infinite DOF, this technique features an improved resolution and an enhanced image contrast. To demonstrate this, Fig. 4 compares the conventional image of the grid (a) to the image reconstructed by Γ (c). The spatial frequency spectra (b&d) verify that, in contrast to conventional imaging, the 2nd harmonic frequency can be observed using the presented system.
To prove the infinite DOF, the grid was imaged for different Δz. Fig. 5 shows the influence of this defocus on the conventional system compared to the interferometric one. While the conventional images blurs with an increased Δz, the images reconstructed by Γ remain sharp.

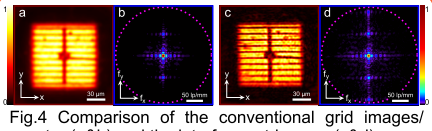

Fig.4 Comparison of the conventional grid images/ spectra (a&b) and the interferometric ones (c&d).

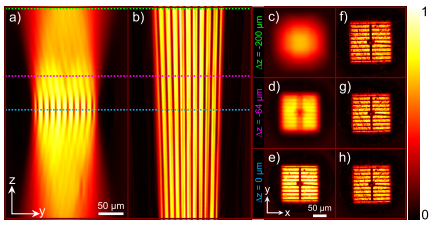

Fig.5 y-z cross sections of Δz-image stacks (a&b) and the x-y-images at the positions indicated by the dashed lines (c-h).

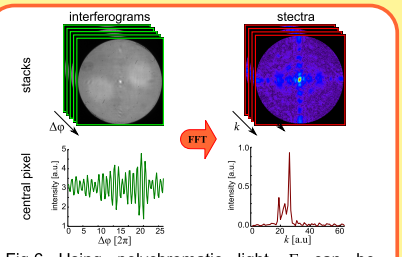

Fig.6 Using polychromatic light, Γ can be obtained from various interferograms

If polychromatic light is used, methods using approaches from Fourier spectroscopy can be applied to gain Γ. Therefore, one mirror of the III is moved by a PA. While varying the optical path difference, various interferograms are acquired. By the Fourier transform of this image stack, Γ for different wave lengths can be obtained (Fig. 6). Hence, it is possible to reconstruct object structures at different wave lengths.
Fig. 8 presents the images gained by the illumination system shown in Fig. 7. Besides the different colors, the three object structures also have different distances Δz to the focal plane.
Using coherence imaging microscopy, all planes are reconstructed sharply and the colors are reproduced correctly.

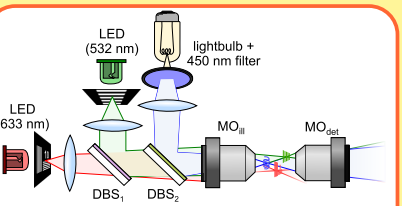

Fig.7 Scheme of the illumination system using three different colors. The structures are imaged into different planes as well.

Conclusion

It is shown, coherence imaging microscopy is an appropriate method to gain an infinite DOF. Furthermore, due to the modified PSF, the imaging quality is enhanced compared to conventional wide-field microscopy.
Using various interferograms, it is possible to obtain color information as well. The spectral resolution and the bandwidth are correlated to the amount of interferograms and the maximal optical path length difference.

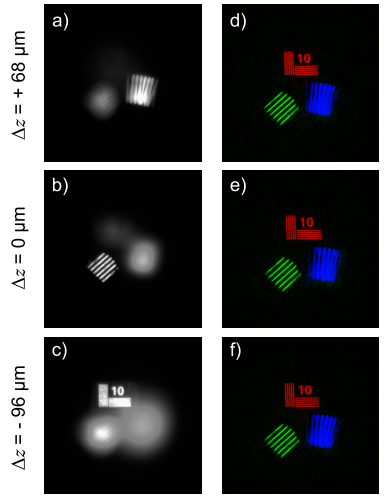

Fig.8 (a-c) Conventional images, acquired at different Δz and reconstructed color images at the same distance to the focal plane.

[1] D.Weigel, A. Kiessling, and R. Kowarschik, "Verfahren zur hochaufgelösten Messung des komplexen Kohärenzgrades" 114. Jahrestagung der DGaO, 2013, P23

[2] D.Weigel, H. Babovsky, A. Kiessling, and R. Kowarschik, "Widefield microscopy with infinite depth of field and enhanced lateral resolution based on an image inverting interferometer," Opt. Commun. 342, 102–108 (2015)

DGaO-Proceedings 2015 - http://www.dgao-proceedings.de - ISSN: 1614-8436 - urn:nbn:de:0287-2015-P031-8
submitted: 19.06.2015 published: 21.08.2015